Article

Nonisothermal Evaporation of Sessile Drops of Aqueous Solutions with Surfactant

Sergey Misyura [1,*], Andrey Semenov [1,2], Yulia Peschenyuk [1,2], Ivan Vozhakov [1,2] and Vladimir Morozov [1]

1   Kutateladze Institute of Thermophysics SB RAS, 630090 Novosibirsk, Russia
2   Faculty of Physics, Novosibirsk State University, 630090 Novosibirsk, Russia
*   Correspondence: misura@itp.nsc.ru

Abstract: In recent decades, electronic devices have tended towards miniaturization, which necessitates the development of new cooling systems. Droplet cooling on a heated wall is effectively used in power devices with high heat flux densities. The use of a surfactant leads to an increase in the diameter of the wetted spot and the rate of droplet evaporation. Despite the wide interest and numerous works in this area, there are still unexplored questions regarding the influence of surfactant and wall temperature on convection, of nonisothermality, and of the decrease in the partial pressure of vapor with increasing surfactant concentration. This work experimentally studies the effect on the rate of droplet evaporation of wall temperature in the range 20–90 °C and of the concentration of surfactant in an aqueous solution of sodium lauryl sulfate (SLS) from 0 to 10,000 ppm. It is shown for the first time that an inversion of the evaporation rate related to the droplet diameter occurs with increasing wall temperature. The influence of key factors on the evaporation of a water droplet with SLS changes with temperature. Thus, at a slightly heated wall, the growth of the droplet diameter becomes predominant. At high heat flux, the role of nonisothermality is predominant. To determine the individual influence of the surfactant on the partial pressure of water vapor, experiments on the evaporation of a liquid layer were carried out. The obtained results and simplified estimates may be used to develop existing calculation models, as well as to optimize technologies for cooling highly heated surfaces.

Keywords: droplet evaporation; heated wall; surfactant; heat transfer; free convection

1. Introduction

In the modern world, the main tasks of technical design, such as weight reduction and object miniaturization, face implementation problems due to the disadvantages of conventional heat removal systems. Efficient dissipation of high heat fluxes requires new approaches to cooling [1]. At present, various two-phase heat exchangers such as spray systems [2], film cooling [3], and microchannel heat exchangers [4] are being widely investigated. In addition, some researchers are considering the possibility of changing the properties of the working fluid with the help of various additives [5,6].

One of the new directions in the study of the effectiveness of cooling systems is the use of aqueous solutions with surfactants as a working fluid [7]. However, the addition of a surfactant can reduce the liquid evaporation rate, leading to a decrease in the equipment efficiency. The easiest way to find out the influence of this factor is to study the evaporation of an immobile sessile drop. The problem of an evaporating drop has attracted the attention of researchers since the end of the last century. A well-known problem is that of the "coffee drop" [8]: the drop is deposited on a rough substrate and its contact line remains stationary during evaporation, when the capillary flow carries the material from the center to the edge and, on drying, results in a circular trail. Another case is when the drops are applied to a smooth, well-wettable surface. In this case, the drop spreads, i.e., the contact line is movable [9,10].

The theoretical description of evaporating droplets is complicated by a large number of physical effects that must be taken into account. The problem of droplet spreading and evaporation is the subject of many works, which are summarized in a sound review by Bonn et al. [11]. In the classical mathematical formulation of the mass transfer model in single-component spherical droplets evaporating in still air, Maxwell's approach was used [12]. It was assumed that the ratio of diffusion time to evaporation time $R_d^2/D_v\tau_e \approx \rho_{vs}(1 - RH)/\rho_a$ is small, and then evaporation may be considered as a quasi-stationary process. In this case, the mass flow is limited by diffusion and for a spherical drop, it is equal to:

$$J_M = 4\pi R_d D_v(\rho_{vs} - \rho_{va})$$

Assuming that the vapor obeys the ideal gas law, the vapor density can be expressed in terms of the partial pressure:

$$\rho_v = \frac{p_v M_v}{RT} = \frac{RHP_{sat}(T)M_v}{RT}$$

In the case of evaporation of a liquid drop in air, the resulting vapor on the droplet surface displaces the surrounding vapor-air mixture and forces it to move away from the drop at a certain velocity. This phenomenon is called the Stefan flow. The evaporation rate of a spherical droplet is limited by the Stefan flow [13]:

$$J_S = 4\pi R_d D_v \rho_a ln(1 + B_M)$$
$$B_M = (\rho_{vs} - \rho_{va})/(\rho_a - \rho_{vs})$$

Tonini and Cossali [14] extended this model to the case of nonisothermal evaporation of a spherical drop in the surrounding atmosphere.

When considering small sessile drops with a contact radius less than the capillary length $\lambda_c = \sqrt{\sigma/\rho_l g}$, the gravitational forces are insignificant, so the liquid takes the form of a spherical cap. The height h_d, surface area S_d and volume V_d of a spherical cap can be calculated using the wet spot radius R_d and the contact angle θ:

$$h_d = R_d tan(\theta/2)$$
$$S_d = \pi(h_d^2 + R_d^2)$$
$$V_d = \frac{\pi h_d}{6}(3R_d^2 + h_d^2)$$

Hu and Larsen [15] developed an isothermal evaporation model for a sessile drop. An analytical dependence of the mass flow on the contact angle was obtained. The developed theory is in good agreement with the experimental data and the results of numerical calculations for contact angles from 0 to $\pi/2$. According to this model, the mass flow is:

$$J_H = \pi R_d D_v(\rho_{vs} - \rho_{va})(0.27\theta^2 + 1.3)$$

Experimental studies of the evaporation of a sessile drop have been carried out for a long time and have resulted in extensive and versatile data. The papers [16–18] deal with water drop evaporation in the open air, showing the influence of such parameters as substrate material, angle of inclination, and environmental conditions on the evaporation process. By now, a relatively large amount of information on the evaporation of various liquids has been collected.

Tarasevich [19] performed an analytical analysis of hydrodynamics inside a sessile drop at the initial stage of evaporation. The qualitative picture of the velocity field was shown to be independent of the ratio between the drop height and the radius of the contact line. Saada et al. [20] numerically simulated the evaporation of a drop lying on a heated substrate. The simulation took into account the convection of the surrounding air as a result of heating from the substrate, but heat was considered to be transferred inside the drop only due to thermal conduction. The results revealed an underestimation of the evaporation

rate compared to the experimental data, and the error increased with increasing substrate temperature. Timm et al. [21] presented data on the evaporation rate in comparison with the diffusion dependence. This assumption was shown to be valid when the time scale of vapor concentration diffusion was much smaller than the total time of droplet evaporation. However, these conditions are valid for experiments in open air.

Misyura [22] demonstrated that at high corrosion rates and intense gas evolution, the evaporation rate decreases due to a decrease in the rate of heat supply to the droplet surface. Modeling the corrosion kinetics also requires taking into account the statistical nature of the corrosion process, which depends on the wettability and droplet diameter. It was shown for the first time that the corrosion kinetics is determined by the wetting regimes. Misyura et al. [23] also studied the effect of the thermocapillary convection and surfactant in a sessile droplet during nonisothermal evaporation.

Misyura [24] investigated the influence of the free convection. The Marangoni thermal convection was shown to play a predominant role in the heat transfer in the liquid evaporation.

Truskett and Stebe [25] investigated the effect of an insoluble surfactant monolayer on the evaporation rate. In this work, no difference from pure water was found. Kim et al. [26] studied the flash evaporation of water droplets with the addition of a surfactant. The latter was shown to strongly affect the shape of the evaporating droplet due to Marangoni forces. Semenov et al. [27] conducted an experimental and theoretical study of the contact angle during the evaporation of drops with surfactant solutions. Guti'errez et al. [28] proved that during vacuum evaporation, a surfactant reduces the rate of water evaporation.

For normal liquids, in particular pure water and most aqueous surfactant solutions [29], the surface tension decreases with increasing temperature. This means that the derivative of the surface tension coefficient with respect to temperature is negative. Hence, thermocapillary Marangoni forces arise with a nonuniform temperature distribution on the surface. The result is an outflow of fluid from warm area to cold area.

The term "self-wetting" was introduced by Abe et al. [30], who studied the thermophysical properties of dilute aqueous solutions of high-carbon alcohols. Due to thermocapillary stresses and the shape of the surface tension–temperature curve, the investigated liquids spread in a "self-wetting" manner, spontaneously propagating towards hot areas, and thereby preventing hot surfaces from drying out and increasing the rate of heat transfer. Because of these properties, "self-wetting" liquids were associated with significantly higher critical heat fluxes compared to water [31]. Savino et al. studied the behavior of vapor locks inside wickless heat pipes [32]. They found that the plugs were significantly smaller than those of liquids such as water. The study of self-wetting liquids was carried out in microgravity for space applications on the International Space Station [33]. Hu et al. [34] demonstrated that the use of these fluids in micro-oscillatory heat pipes resulted in an increase in heat pipe efficiency.

The use of alcoholic solutions with water may be undesirable, since they can significantly differ in thermophysical properties from pure water. At the same time, a very small amount of this substance is used for creating a surfactant solution, which does not affect its thermophysical properties, but noticeably changes its surface properties.

The performed analysis of existing works has shown that there are very few experimental and theoretical data on the influence of various factors on the evaporation of a drop of an aqueous solution with surfactant in a wide range of wall temperatures. The complexity of these studies is related to the fact that at high-temperature evaporation, the isothermal model of diffusion is unacceptable and evaporation is influenced simultaneously by many key factors. In addition, the properties of the surfactant change strongly with increasing liquid temperature.

Previous experimental studies have demonstrated that the addition of a surfactant leads to a decrease in the evaporation rate of a liquid droplet. However, the specific factors influenced by the surfactant have not been established. In addition, there has been no

comprehensive study of the effect of the surfactant in a wide range of wall temperatures and droplet base diameters.

Research objectives of this article are as follows. (1) Experimental determination of geometrical parameters of a droplet and measurement of temperature fields of a liquid droplet. The obtained experimental data are used to predict the evaporative behavior of droplets in a wide range of wall temperatures. (2) On the basis of experimental data, approximate calculations are made to estimate the influence of separate key factors on the droplet evaporation rate. The findings may be useful for the development of the existing models for determining the evaporation rate of droplets of solutions with surfactants, which is important for the creation of droplet irrigation technologies, widely used for heat exchange intensification in devices with high energy efficiency.

2. Experimental Setup

Preparation for the experimental study of droplet evaporation involved obtaining aqueous solutions with surfactants. In the presented work, three different surfactants were selected: polyoxyethylene sorbitan monooleate (TWEEN 80), cetrimonium bromide (CTAB), and sodium lauryl sulfate (SLS). They differed in properties depending on the charge component of their hydrophilic components: nonionic (TWIN80), cationic (CTAB), or anionic (SLS).

Using a high-precision micro analytical balance AND BM-252 with a readability of 0.01 mg, the weight of the surfactant was measured. It was then mixed with deionized nanofiltered Milli-Q pure water, and the solution was thoroughly stirred at room temperature in a closed cuvette, using a magnetic stirrer with medium speed.

Attempts to obtain an aqueous solution of TWIN80 have demonstrated that producing the solutions of nonionic surfactants requires a special procedure, described in chemical protocols, including special conditions and additional reagents. Concluding that TWIN80 is poorly soluble in water, it was decided not to use it for our experiments. The study of the remaining solutions is carried out using two experimental setups described below.

2.1. Tensiometer KRÜSS K100

The analysis of the properties of aqueous solutions with surfactants was carried out on a precision tensiometer KRÜSS K100 with KRÜSS laboratory software. Using a Huber thermostat, a cuvette with a working liquid was heated or cooled in the temperature range from 294 K to 343 K. Measurements were performed using the Wilhelmy plate method. A standard 10 mm × 20 mm × 0.2 mm platinum plate was used to measure surface tension since the contact angle of such a plate with most liquids is approximately zero. The second plate with dimensions of 10 mm × 20 mm × 2.8 mm was made of copper of industrial grade A1 and was used to measure contact angles. The copper surface was technically treated. In most cases, copper with high thermal conductivity and low cost is used as a main material for heat pipes. In the case of using a nonstandard plate, a special holder was used to ensure a strictly vertical position for the copper plate.

The tensiometer placed the platinum strip in the solution, then slowly removed it at a constant rate until it was completely out of the solution. During this procedure, the tensiometer measured the force f with which the plate was removed. Furthermore, the value of the surface tension coefficient σ was calculated by the formula: $\sigma = f / (l \cdot cos\theta)$.

In this case, the contact angle θ between the platinum plate and the investigated fluid was taken to be zero. To measure the value of the contact angle with the copper plate, a similar procedure was followed. To verify the obtained data, measurements were carried out in series of 5 runs. As a result, statistically averaged data for the surface tension coefficient $\sigma(T)$ and the contact angle θ were obtained.

2.2. Drop Shape Analyzer KRÜSS DSA100

Experiments for the sessile liquid drop evaporation were performed with the use of the DSA100 drop shape analysis system, produced by KRÜSS and presented in Figure 1.

This device consists of three main parts: a high-precision dosing system with the dosing step of 0.1 µL, a motorized object table with program-driven movement in 2 horizontal axes, and the optical shadow system which includes a 50 W light source and a CCD camera with a resolution of 780 × 580 pixels (field of view varied from 3.7 mm × 2.7 mm to 23.2 mm × 17.2 mm). A Peltier chamber open to the atmosphere was used for heating substrates. It allowed the specified temperature of the bottom wall to be maintained with an accuracy of about 0.1 °C. The thermostat was used to cool the chamber and maintain the temperature of the substrate. The needle with the selected solution was moved into the chamber and a drop was deposited onto the substrate surface.
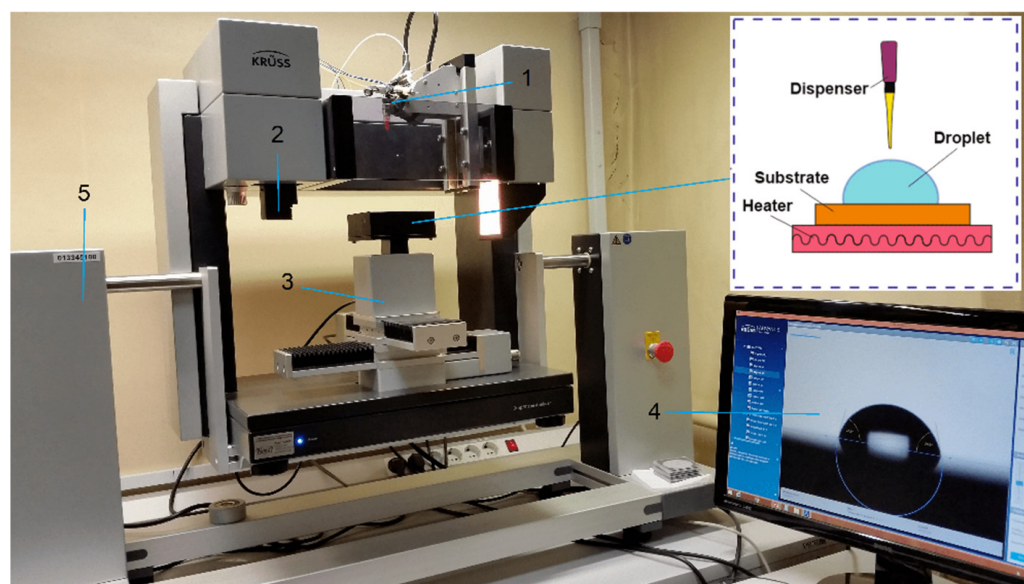

Figure 1. KRÜSS DSA 100 experimental setup: 1—dosing system; 2—camera; 3—three-axis positioning system; 4—processed image of a droplet; 5—automatic inclination system.

Measurement of the surface temperature of the copper substrate was carried out using a platinum resistance thermometer, fixed at the distance of 1–2 mm from the liquid drop. A special platinum resistance thermometer pt100 with a diameter of 2.5 mm, produced by KRÜSS, was applied. The accuracy of pt100 was 1/3 DIN class B (±0.1 °C at 0 °C to 0.8 °C at 400 °C). To increase the reliability of temperature measurements, the wall temperature was also measured by a thermocouple, located at a distance of 0.3–0.5 mm from the surface of the copper substrate on which a droplet was placed. The measurement error for the wall temperature (T_w) made by this thermocouple did not exceed 0.5–1 °C (taking into account the estimated distance of the thermocouple from the wall). The substrate surface temperature in each experiment was kept constant. The temperature and relative humidity of the ambient air during the experiments was 20–21 °C and 30–32%, respectively.

The measurement error of the droplet diameter did not exceed 5%. In the range of contact angle of 90–20°, the inaccuracy of the contact angle of the drop ranged within 3–5%. The maximum error of the evaporation rate did not exceed 5–7%.

The initial liquid drop volume was about 2–3 µL. The KRÜSSDSA Advance software allowed the processing of the shadow images of evaporating liquid droplets in fully automatic mode 2 (real-time determination of the droplet volume, base diameter and contact angles). Figure 2 shows a photograph of the liquid droplet shape analysis.
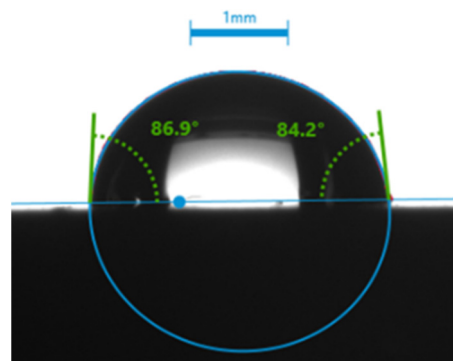
Figure 2. Photograph of liquid droplet shape analysis.

3. Experimental Results

The presented results of the experimental studies are divided into two main parts. To begin with, the analysis of aqueous solutions of SLS and CTAB on the KRÜSS tensiometer is considered. The second part is devoted to the results of the study of droplet evaporation.

3.1. Surface Tension

The wide temperature range specific for the operation of a pulsating heat pipe imposes restrictions on the applicability of working fluids. One of the determining roles in heat transfer and efficient operation of a pulsating heat pipe is played by the properties of the working fluid used.

At the outset, researchers obtained data on the dependence of surface tension on the concentration of surfactants in an aqueous solution at a room temperature of about 20 °C. For this purpose, a wide range of concentrations of surfactant solutions was used. The maximum concentration exceeded the CMC (critical micelle concentration), while the minimum concentration was similar in terms of surface tension to that of pure water. The components of the experimental setup were carefully prepared before each measurement. To reduce contamination caused by the surfactants used, the cuvette for the investigated working fluid was cleaned with a 70% isopropanol solution and washed several times with clean water.

Aqueous solutions with four different concentrations of SLS were investigated and pure water was examined for comparison. Figure 3 shows temperature dependence of surface tension of aqueous solutions with surfactants.
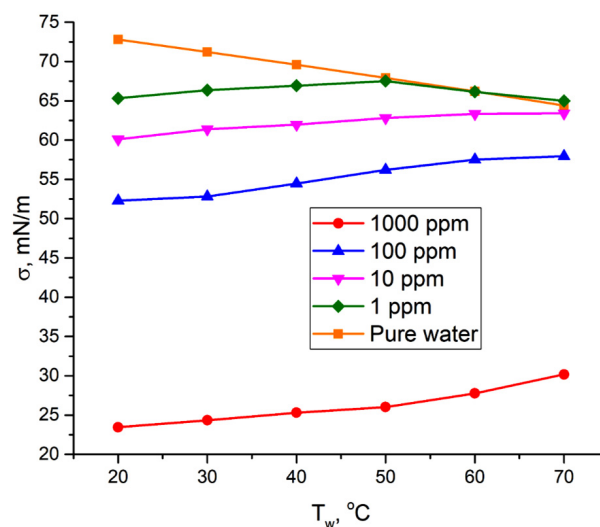

Figure 3. Surface tension vs. temperature for different concentrations of SLS in aqueous solutions.

The general dependence $\sigma(T)$ for CTAB is similar to that for water. That is, the first derivative of surface tension with respect to temperature is less than zero. In a heat exchange facility, for example, such as a pulsating heat pipe, liquid flows from the more heated area to the less heated one occurring on the surface due to Marangoni forces. This leads to the formation of dry spots and a decrease in the heat transfer coefficient, which may lead to overheating of the equipment. However, the SLS solution does not exhibit regular dependence, as CTAB, water and other normal liquids do [35]. Figure 3 shows that $d\sigma/dT$ is positive over a wide range of SLS concentrations. At the same time, it should be noted that at low SLS concentrations, a rapid change in the sign of the derivative is observed with increasing temperature. The temperature of the break point depends on the concentration. At higher temperature, the surface tension of the solution completely coincides with that of water.

Thus, aqueous solutions of SLS have the properties of a self-wetting liquid in a wide range of concentrations and temperatures. However, self-wetting liquids are quite often known to be unstable, which is also confirmed by the results of the current study.

From the obtained data, it may be inferred that SLS solutions are useful in solving the problem of dry spots and expanding the working range into the region of higher heat fluxes—with the proviso, of course, that for each task it is necessary to pay attention to the permissible range of applicability for each specific concentration of the solution.

3.2. Evaporation

In droplet evaporation, it is important to take into account the contact angle, since this determines the shape of the droplet surface. Therefore, the contact angles of evaporating droplets were measured for different concentrations of surfactant solutions and different substrate temperatures.

Figure 4 shows the evolution of a pure water drop during evaporation under isothermal conditions at a room temperature of about 21 °C. Since the drop has a small volume of the order of 1 μL, its shape is a spherical cap. In this case, evaporation apparently occurs at a fixed contact line, with the so-called "pinning" of the contact line. The evaporation is as a result of the diffusion of vapor from the drop surface, where it is saturated, into the atmosphere with a constant vapor concentration (in the experimental conditions, the humidity was about 30–40%). The evaporation is almost uniform over the entire surface area and is well described by Stefan's theoretical model [13]. Droplet evaporation on the heated surface qualitatively coincides with isothermal evaporation, but there are important differences. In this case, the mass flow from the droplet surface is substantially nonuniform. A significant mass flow is provided by intense evaporation in the area of the contact line, called the microregion [36].
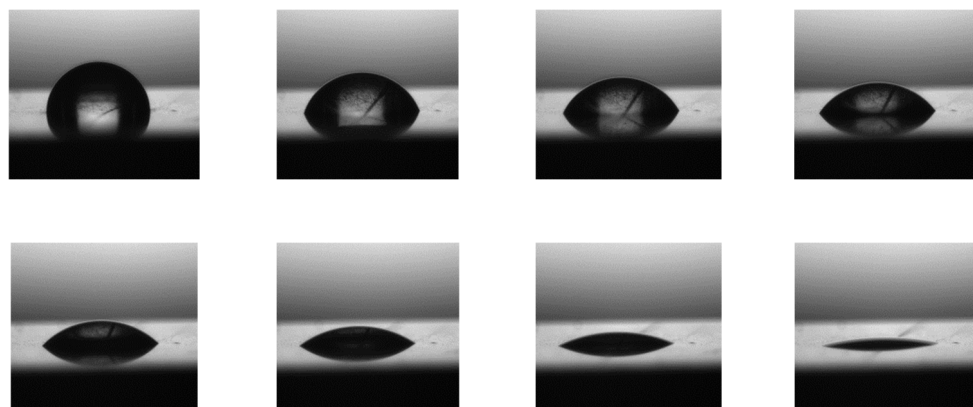

Figure 4. Evolution of an evaporating water droplet at a temperature of 21 °C (the initial droplet radius $R_d = 0.7$mm, the initial contact angle $\theta_0 = 97°$). Time step equals 300 s.

In a further step, the evaporation of drops of surfactant solutions was considered in order to find out the effect of the surfactant concentration on the evaporation rate (heat exchange with the substrate) and the behavior of the contact line during evaporation.

The data for a small set of drops are presented below, whereby all the given graphs of diameter and contact angle correspond to the same drops.

Figures 5 and 6 show values of the droplet contact angle and the droplet height versus time during evaporation. At the initial moment of time, the contact angle of droplets of surfactant solutions is in the range from 35° to 100°. The initial droplet height is 0.4–1 mm. Upon evaporation, the contact angle decreases, which is associated with a change in the droplet volume, but the contact line remains almost immovable. It is clearly seen that pure water corresponds to the maximum contact angle for both low (30 °C) and higher (80 °C) temperatures.
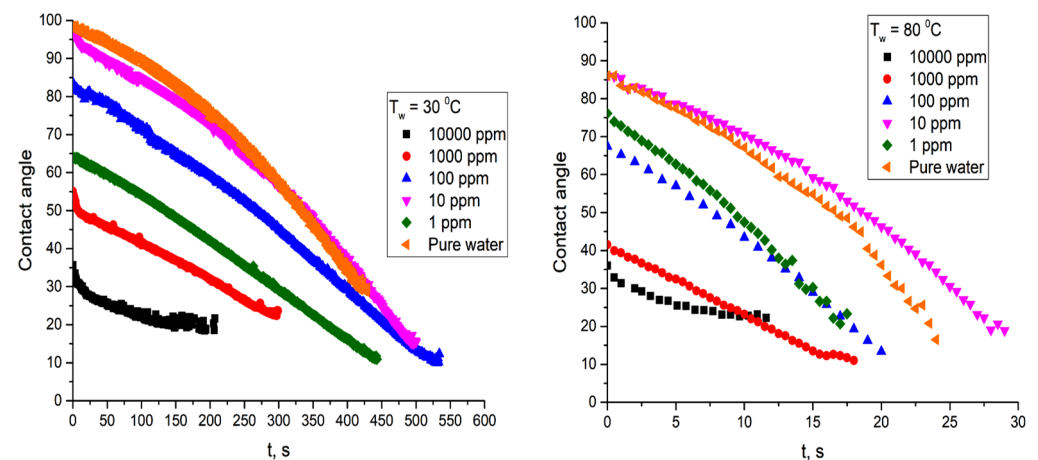
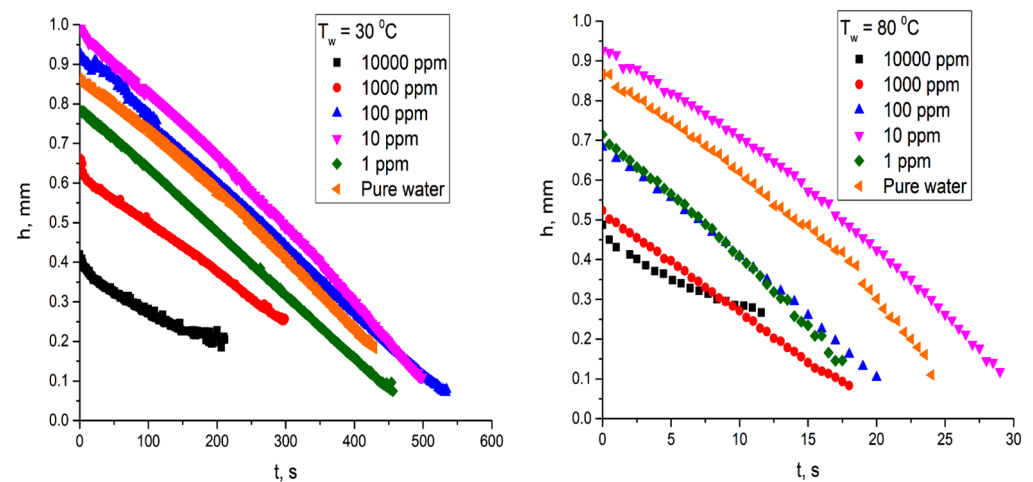**Figure 5.** Evolution of contact angle over time of evaporation.

Figure 6. Evolution of drop height over time of evaporation.

Meanwhile, at a low surfactant concentration, the contact angle does not differ from that of pure water, and with an increase in the surfactant concentration, it monotonically decreases. There are two reasons for this. First, the surface tension reduction leads to a decrease in capillary forces and spreading of the droplet. Secondly, at the initial stage, the temperature of the liquid is close to room temperature and, upon contact with the heated substrate, it begins to heat up rapidly. It is supposed that the drop heating in the vicinity of the contact line occurs faster than in the main volume of the drop, which gives rise to the Marangoni force. The force vector is directed along the surface from lower to higher temperature. Estimating the time required to heat the drop to the substrate temperature,

previous researchers obtained the formula $\tau = R^2 \rho c_p / \lambda \approx 6$ s. Thus, the droplet diameter should grow noticeably in the first seconds of heating.

Figure 7 shows the droplet diameters as a function of time. At low surfactant concentrations in pure water, the diameter is seen to be constant during the entire evaporation time, except for the last seconds of the droplet life.
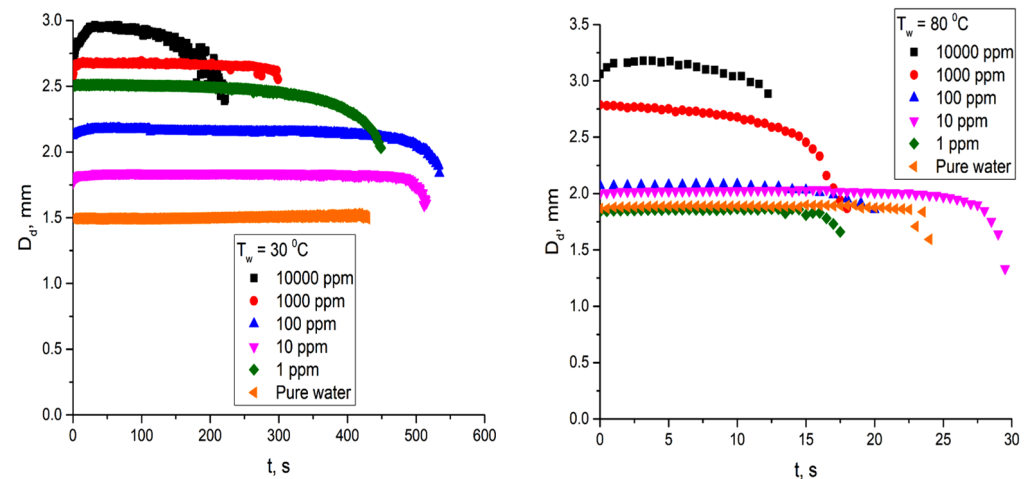

Figure 7. Evolution of dropletsdiameter over time of evaporation.

With increasing concentration, the area where the change in diameter occurs is clearly observed to stretch over time. Moreover, for a high concentration (above CMC), the droplet diameter changes throughout the entire evaporation process: in the first seconds, the drop diameter increases as the drop itself spreads, and then decreases as it dries.

4. Predicting the Evaporative Behavior of a Water Droplet with a Surfactant

Direct numerical simulation of the unsteady and nonisothermal evaporation of a water droplet with a surfactant is very complicated due to the large number of uncertain factors that affect each other. In the presence of a surfactant, it is hard to estimate the equilibrium diameter of the droplet, which can change markedly over time when the droplet evaporates. Any change in the diameter, contact angle or height of the droplet alters free convection in the gas and liquid phase. The surfactant affects the partial pressure of water vapor and, accordingly, the evaporation rate. To date, there are no reliable methods for computing all these factors. Calculating the temperature of the free surface of the droplet is extremely difficult, since the Marangoni flow and convection in a droplet depend on the surfactant concentration. Therefore, assessment of the influence of various key factors on the evaporative behavior of the droplet becomes crucial at the first stage. For this purpose, it is advisable to use experimental data on the geometry of the droplet, as well as on the thermal field measured by a thermal imager (T_s) and a thermocouple (T_w).

4.1. Key Factors Effecting the Droplet Evaporation

In general, the rate of evaporation depends on the geometry of the droplet, the conditions of heat transfer and on free convection. It is possible to distinguish the following key parameters that determine the intensity of evaporation of a water droplet with the addition of a surfactant:

(1) Drop diameter;
(2) Natural convection of gas;
(3) Natural convection of liquid;
(4) Nonisothermality;
(5) Buoyancy of water vapor in air and the Stefan flow;
(6) Evaporation rate of surfactant solution.

With a small droplet diameter (1–3 mm) and in the absence of wall or air heating, convection in the liquid and gaseous phases can be neglected. When a droplet evaporates on a hot wall, free convection has to be taken into account. The influence of these key factors on the evaporation of liquid are considered separately below.

(1) Let us take a detailed look at the influence of the wetted droplet diameter on the evaporation rate. In most experimental curves, there is an attached contact line for most of the evaporation time (evaporation mode of constant contact radius, or CCR). With the growth of the surfactant concentration, the droplet radius increases. Despite the decrease in the contact angle with time, for most of the curves, a quasi-linear decrease in the droplet volume is realized (i.e., at a fixed radius, the evaporation rate (dV/dt) is constant, despite a significant decrease in θ). Thus, the effect of the surfactant on evaporation due to the change in radius will be proportional to the ratio of the radii of the two drops ($J_1/J_2 \sim R_{d1}/R_{d2}$). To analyze the influence of other key factors, it is necessary to exclude the influence of the radius being a part of the ratio J/R_d.

(2) Let us estimate the effect of gas convection on the evaporation of a drop. When a liquid layer evaporates, the convective mass flow of water vapor through air can be estimated using Equation (1) [37],

$$Sh = 2 + 0.55(Re)^{0.5}(Sc)^{0.33} \tag{1}$$

where the Sherwood number $Sh = \beta R_d/D_v$, the Schmidt number $Sc = \nu_g/D_v$, the Reynolds number $Re = U_{ca}R_d/\nu_g$, in which β is the mass transfer coefficient, R_d is the radius of the droplet, D_v is the diffusion coefficient of water vapor in air, U_{ca} is the rate of thermogravitational convection of air at the temperature difference (ΔT_s) between the temperature of the free surface of the droplet T_s and the temperature of the ambient air T_a, and ν_g is the kinematic viscosity of the gas. The evaporation rate J is related to the mass transfer coefficient through the concentration difference $\rho_{vs} - \rho_{va}$ given in Equation (2),

$$J = \beta F(\rho_{vs} - \rho_{va}) \tag{2}$$

where F is the interface area of the layer.

For intense convection, when the Sherwood number is much greater than 1, $Sh = 0.55(Re)^{0.5}(Sc)^{0.33}$, then in accordance with Equations (1) and (2),

$$J \sim \beta \sim (U_{ca})^{0.5} \tag{3}$$

The air velocity due to thermogravitational convection can be approximated from Equation (4),

$$U_{ca} \sim (g\beta\Delta T_s R)^{0.5} \tag{4}$$

and the evaporation rate is related to the droplet radius according to Equation (5):

$$J \sim (R_d)^{0.5} \tag{5}$$

As indicated in Equation (5), the presence of the surfactant leads to an increase in the droplet radius; and an increase in the radius contributes to an increase in evaporation.

(3, 4) Let us evaluate the joint influence of factors 3 and 4, since they are interrelated. For convenience of analysis, the effect of these factors will be denoted as the effect of nonisothermality. The heat flux in the liquid q_l is supplied to the interface of the drop and spent on evaporation ($q_e = rJ$, $J = \Delta m/\Delta t$), radiation ($q_r = \varepsilon\sigma(T^4_s - T^4_a)$) and free air convection ($q_c = \alpha_a(T_s - T_a)$). The heat balance for the droplet surface corresponds to Equation (6),

$$q_l = q_e + q_r + q_c = rJ/F + \varepsilon\sigma\left(T^4_s - T^4_a\right) + \alpha_a(T_s - T_a) \tag{6}$$

where r is the latent heat of vaporization, and F is the area of the liquid interface. The air heat transfer coefficient α_a is determined by the Nusselt number $Nu = \alpha_a R_d / \lambda_a = 0.54\, Ra^{0.2}$, where Ra is the Rayleigh number [37]. The heat supplied to the liquid from the wall is determined by the conductive and convective heat transfer in the liquid according to Equation (7) [38–40],

$$q_l = \alpha_l(T_w - T_s)$$

$$\alpha_l = \frac{\lambda_l}{h}\left(\frac{U_{cl}h}{a_l} + 1\right)^{0.3} \sim \frac{\lambda_l}{h}\left(\frac{kh^2}{a_l} + 1\right)^{0.3} \sim \frac{1}{h^{0.4}}, \text{ if } \frac{U_{cl}h}{a_l} \gg 1$$

$$\alpha_l = \frac{\lambda_l}{h}\left(\frac{U_{cl}h}{a_l} + 1\right)^{0.3} \sim \frac{\lambda_l}{h}\left(\frac{kh^2}{a_l} + 1\right)^{0.3} \sim \frac{1}{h}, \text{ if } \frac{U_{cl}h}{a_l} \ll 1$$

(7)

where α_l is the liquid heat transfer coefficient, $U_{cl} \sim c(Ma + Ra)$, U_l is the average convective velocity in the liquid droplet, the Marangoni number $Ma = (\Delta T_w h / \mu_l a_l)(d\sigma/dT_s)$, the Rayleigh number $Ra = g\beta_T \Delta T_w h^3 / \nu_l a_l$, β_T is the thermal liquid expansion, g is the gravity acceleration, $\Delta T_w = T_w - T_s$, ν_l is the water kinematic viscosity, a_l is the liquid thermal diffusivity, and μL is the water dynamic viscosity. Empirical expressions for evaporation intensification with an increase in the Ra number are given in [41]. For very small droplets (droplet height below 1 mm), low values of Ra and Ma and low values of U_l are realized, and the condition $\alpha_l \sim 1/h$ (conductive heat transfer) is satisfied. Therefore, the ratio of heat fluxes for a pure water drop (q_{l1}) to a water drop with surfactant (q_{l2}) will be inversely proportional to the ratio of heights $q_{l1}/q_{l2} \sim h_2/h_1$. To determine the relationship between ΔT_w and the heat flux, it is necessary to solve a system of differential equations and it is difficult to make a simplified estimate for the change in $\Delta\rho_s$ due to nonisothermality. Therefore, the effect of nonisothermality can only be determined after the evaluation of other parameters (key factors 1, 2, 5, 6) and taking into account experimental data. At different wall temperatures, the droplet free surface temperature and ρ_s were determined using thermal imaging measurements and the equilibrium curve for the equilibrium partial pressure of water vapor.

(5) Let us consider the effect of water vapor buoyancy. Since water vapor is lighter than air, the effect of the additional flow must be considered. The vapor convection velocity U_ρ corresponds to Equations (8) and (9) [42],

$$U_\rho = ((\rho_a - \rho_m)gL/\rho_m)^{0.5} \tag{8}$$

$$\rho_m = \rho_a - (\rho_a - \rho_v)/\rho_v)C_{cat}(T_a) \tag{9}$$

where ρ_a is the density of the air, ρ_v is the density of the vapor, ρ_m is the density of the air + vapor mixture, and L is the characteristic length of the diffusion vapor layer. Experimental and calculated data in [42] show that the increase in the evaporation rate due to the buoyancy of water vapor (for a wall with high thermal conductivity) is about 40%. It does not depend on the droplet radius ($R_d > 0.8$ mm). Thus, despite the change in droplet diameter due to the surfactant, the effect of buoyancy on J will be the same for a water droplet with and without surfactant.

(6) Let us consider the influence of the surfactant on the droplet evaporation rate. Since the surfactant alters the radius of the drop, the simultaneous influence of several factors appears. To eliminate the effect of the droplet radius, one may consider the evaporation of a water layer (with and without surfactant). According to Equation (10),

$$J = \pi R_d D_v (\rho_{vs} - \rho_{va})(0.27\theta^2 + 1.3) \tag{10}$$

at zero contact angle, the evaporation rate does not depend on the angle: in this case, the expression for evaporation of the liquid layer thus coincides with the expression for a droplet with a very small height, Equation (11):

$$J = 4.1 R_d D_v (\rho_{vs} - \rho_{va}) \tag{11}$$

4.2. Evaporation of a Layer of Water with Surfactant

Figure 8 presents experimental data on the evaporation of a layer of water with (10,000 ppm) and without surfactant. Figure 8a,b gives experimental curves for layer evaporation of $T_w = 21$ °C, and $T_w = 90$ °C, respectively. All curves demonstrate a linear dependence of the layer mass on time.

(a)

(b)
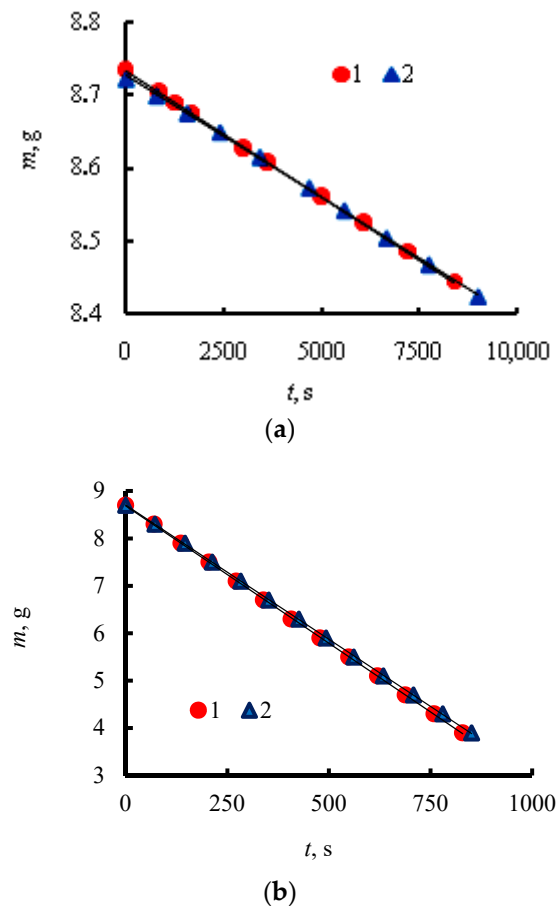
Figure 8. Evaporation of water layer (curve 1) and water layer with 10,000 ppm surfactant (curve 2) for layer diameter 40 mm and air humidity 30%: (**a**) $T_w = T_a = 21$ °C, (**b**) $T_w = 90$ °C, $T_a = 21$ °C.

The measurement of the water layer mass is carried out using the gravimetric method. The working section made of copper with a layer of liquid is placed on the scales. The wall temperature is measured with a thermocouple. Although the cell radius is constant (40 mm), the characteristic radius R_d in Equation (11) is different according to the scenario considered. In the case of water and surfactant, the length of the meniscus on the side wall of the cuvette is greater than for pure water, and the total radius R_{d1} is thus larger than for the water layer by about 11–12% at $T_w = 21$ °C and by 9–10% at $T_w = 90$ °C. Thus, to simplify the variables to a single radius when calculating the evaporation rate of the water with surfactant layer, it is necessary to divide the value of J/R_d by 1.11–1.12 and 1.09–1.1 (taking into account the length of the meniscus).

Figure 9 shows thermal images of the liquid layer and the profiles of T_s along the line $0L$. The average surface temperature T_s of the layer increases during evaporation due to the decrease in layer height. The central region temperature is lower than at the edges. For a water layer with surfactant, the average temperature over the layer surface is higher than the temperature for a pure water layer.
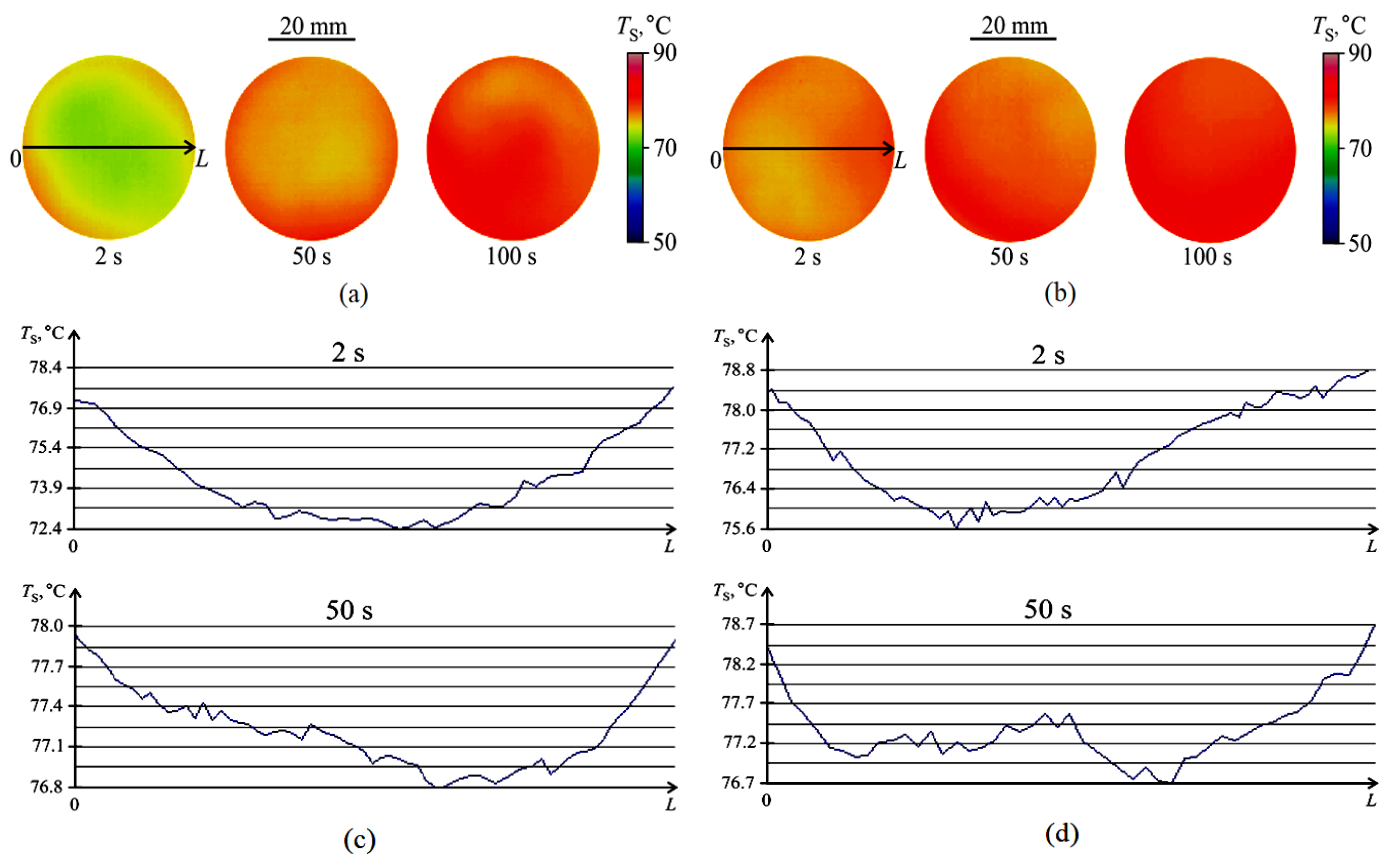
Figure 9. Thermal images of the layer interface of (**a**) pure water and (**b**) the surfactant solution. Temperature profiles of T_s along the $0L$ line for (**c**) the water layer and (**d**) the surfactant solution layer, (**a–d**) $T_w = 90\,°C$, $T_a = 21\,°C$.

4.3. Thermal Imaging Measurements of the Free Surface of a Water Droplet with and without Surfactant

A droplet of water with surfactant shows a 15–20% decrease in J_ρ (compared to pure water) at $T_w = 21\,°C$ and a 9–11% decrease at $T_w = 90\,°C$. The obtained data correspond to the previously obtained measurements in other works. In [43], the maximum decrease in the rate of droplet evaporation with a surfactant is 25–30%. The presence of surfactant also leads to a decrease in J_ρ for the liquid layer [44]. The decrease in J_ρ is due to the competing effect of two factors—a decrease in the instantaneous area of the free surface of a drop occupied by water molecules, and a weakening of the molecular bonds between water molecules and surfactant molecules. The integral value of the two parameters for the entire free surface of the liquid decreases the equilibrium partial pressure of water vapor ρ_{vs} and, in accordance with Equation (11), the evaporation rate.

To assess the influence of nonisothermality, the temperature of the free surface of the drop T_s was measured using a thermal imager and an optical lens providing a tenfold increase in the image (Figure 10a). Evaporation leads to a decrease in T_s. The minimum drop temperature corresponds to the maximum height, i.e., the center of the drop (Figure 10b). Since the diameter of the water with surfactant drop is 1.8–2 times larger than the pure water drop diameter, the height is significantly less. As a result, the temperature difference $\Delta T_w = T_w - T_s$ is lower by 0.4–0.7 °C for a water with surfactant droplet than for water alone. In other words, a drop with a lower height has higher values of T_s and J_T. When adding a surfactant, the increase in J_T (the effect of nonisothermality) is 2–3%.
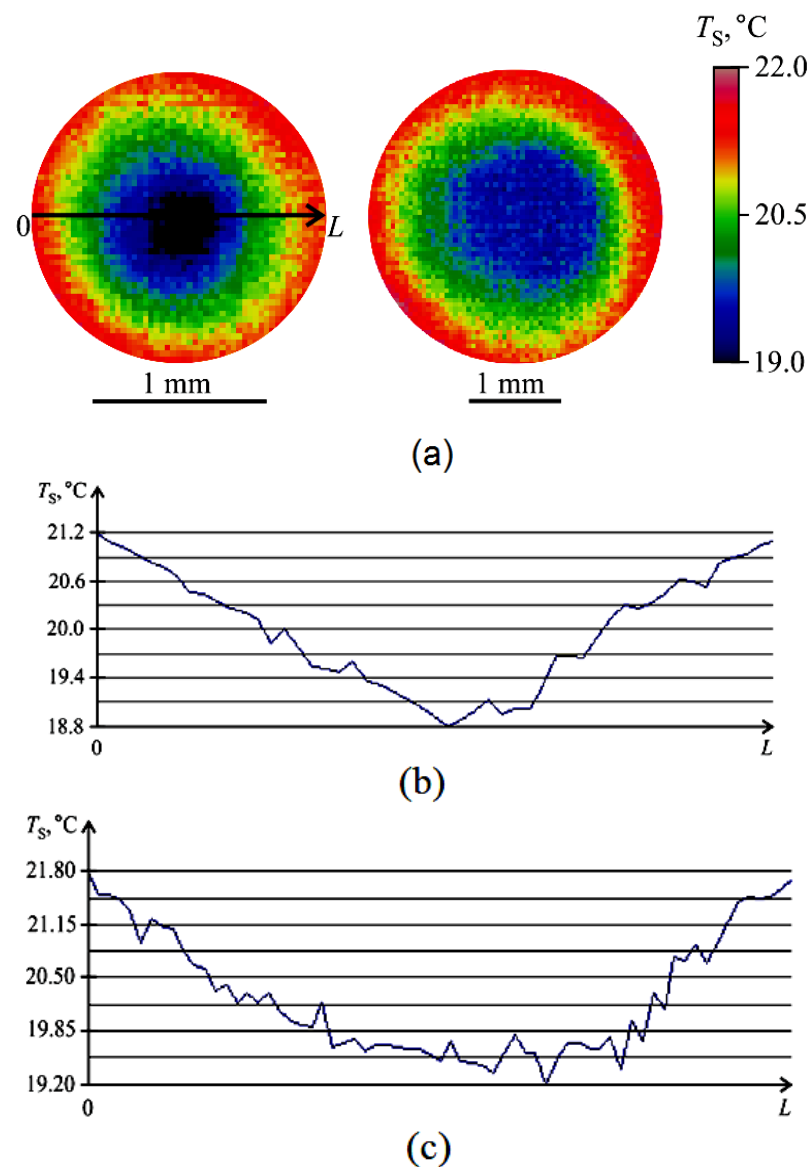
Figure 10. (**a**) Thermal images of the droplet interface for $t = 20$ s (without heating): water is on the left; water with surfactant (10,000 ppm) is on the right; and temperature profiles of the droplet interface at a cross section of 0L: (**b**) water; (**c**)-water with surfactant (10,000 ppm).

With high temperature heating ($T_w = 90$ °C), the droplet diameter increases by 50–60% due to the addition of surfactant. Due to the fast evaporation rate on the heated wall, the temperature T_s depends much more on the drop height. For a water with surfactant droplet, the average temperature T_s (Figures 11 and 12 for $t = 7$ s) for the droplet surface is 4–5 °C higher than that for water during almost the entire evaporation time. This effect of nonisothermality (J_T) leads to a 14–17% increase in the evaporation rate of a droplet of water with surfactant, compared to a pure water drop (according to the water vapor equilibrium curve). Figures 11 and 12 show thermal images of the surface of a drop located on a heated wall, as well as temperature distributions of T_s along the 0L axis. As the wall temperature and T_s increase, the difference ΔT_s increases (comparison with Figure 10a). The small height of the drop and the high heat flux from the wall contribute to the temperature field uniformity over the drop surface.
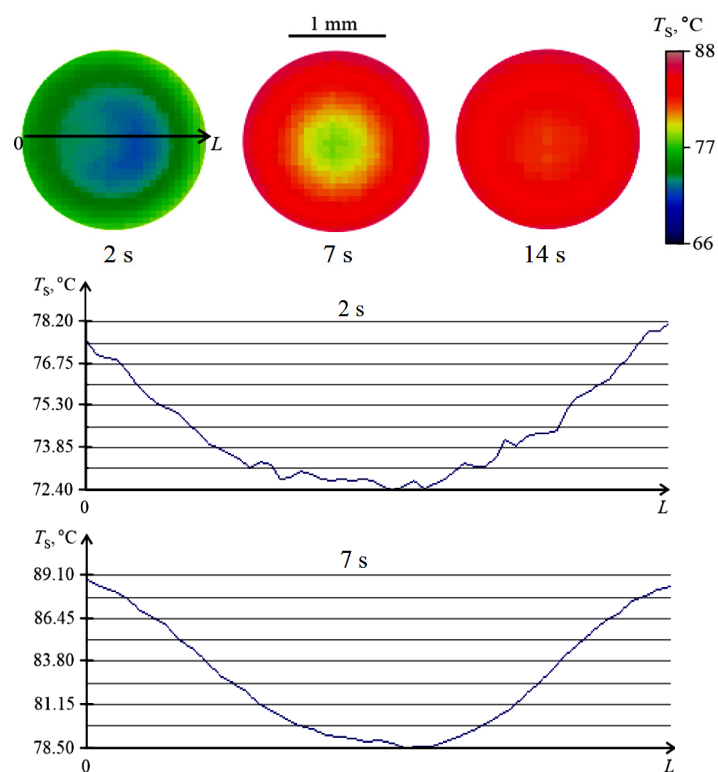
Figure 11. Thermal images of the water droplet interface and temperature profiles of the droplet interface at the cross section of $0L$ ($T_w = 90$ °C).

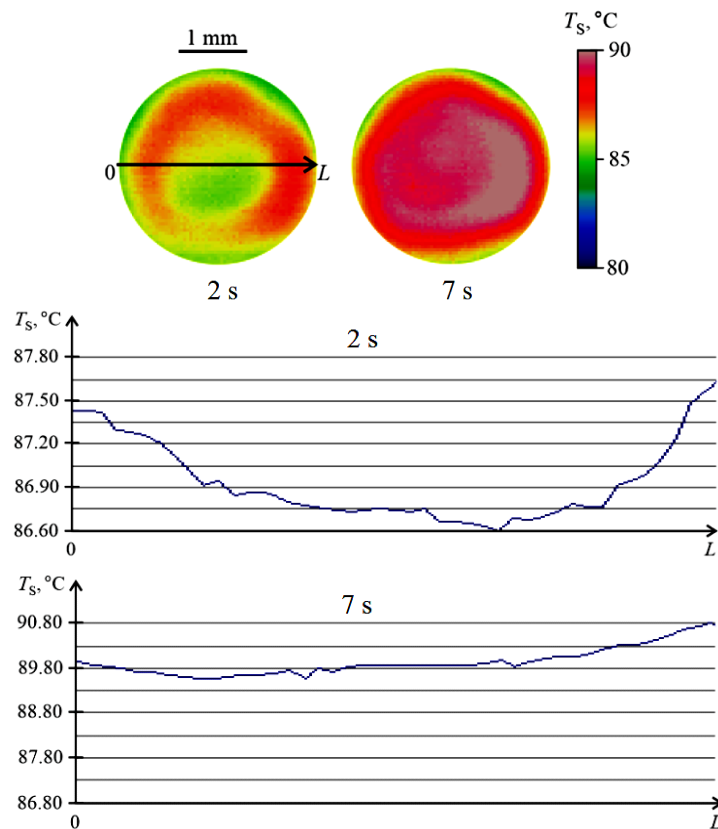**Figure 12.** Thermal images of the droplet interface and temperature profiles at the cross section of $0L$ ($T_w = 91$ °C, water with surfactant at 10,000 ppm concentration).

The temperature profile of the droplet surface at a high wall temperature (T_w = 90 °C) is qualitatively similar to that at an unheated wall. (Figure 10b). The minimum temperature is at the center of the drop and the maximum temperature is at the edges. This distribution is associated with a negligible effect of free convection in the liquid, i.e., the temperature field is determined by the conductive heat transfer due to the small values of the Rayleigh numbers. In this case, the temperature T_s is determined by the height of the droplet ($T_s \sim 1/h$). The surfactant results in a higher temperature T_s and a more uniform temperature distribution over the droplet surface.

4.4. Assessing the Impact of Key Factors on Evaporation of the Water Droplet with Surfactant

To evaluate the effect of several factors on droplet evaporation, it is convenient to exclude the influence of the droplet base diameter, which strongly depends on the surfactant. For this purpose, it is convenient to attribute the value of the evaporation rate to the diameter of the droplet.

Figure 13 provides experimental data on the dependence of $J/2R_d$ on the wall temperature T_w. Points are given for pure water (points 1), water with surfactant 1000 ppm (points 2) and water with surfactant 10,000 ppm (points 3).
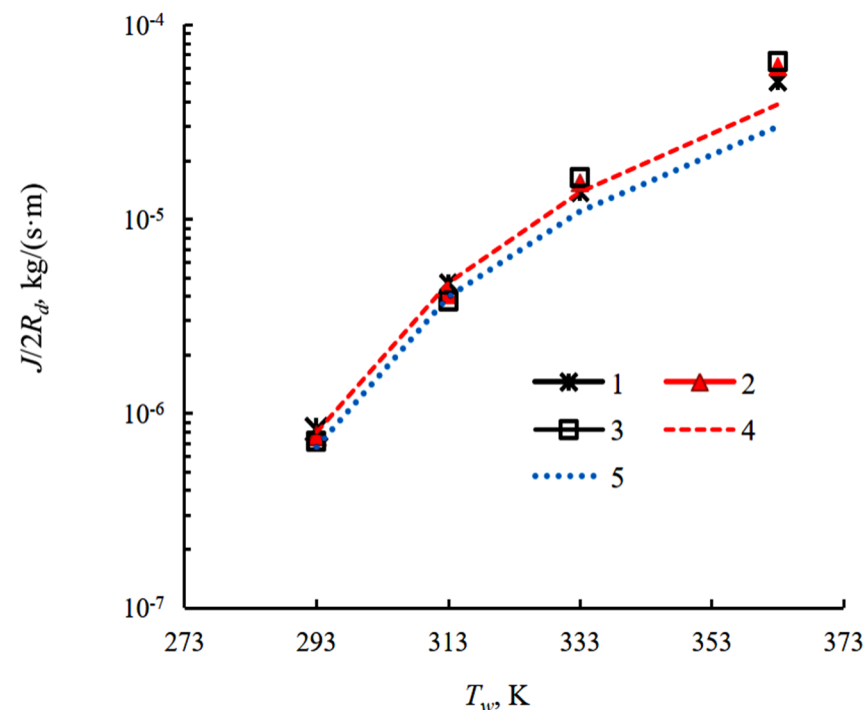

Figure 13. Drop evaporation rate depending on the wall temperature T_w. Experimental results: 1—water, 2—water with surfactant (1000 ppm), 3—water with surfactant (10,000 ppm); and by calculation from Equation (10) for the droplet contact angle: 4—of 60°, and 5— of 27°.

For droplet evaporation at room temperature, as well as at small wall heating (T_w = 313 °K), a water drop evaporates faster than a water with surfactant one (by 14–17% at T_w = 293 °K). At a temperature of T_w = 333 °K, the evaporation rates for points 1–3 are close to each other. At a wall temperature of T_w = 363 °K, a droplet of water with surfactant with a concentration of 10,000 ppm evaporates 25–27% faster. Thus, the simultaneous influence of several factors considered above leads to an inversion of $J/2R_d$ c with increasing temperature. The calculated curve 4 is constructed for the maximum value of the contact angle. This angle corresponds to the experiment with the maximum angle, which is taken as an average value over time ($\theta = (97° + 20°)/2 = 60°$). The curve of angle change over time has a quasi-linear character. Curve 5 is plotted for the lowest contact angle over time ($\theta = (35° + 20°)/2 = 27°$). The drop radius is also taken as the time average in the calculation and processing of the experimental data.

The diffusion coefficient of vapor in air is determined at a temperature $T = (T_s + T_a)/2$, where T_s is the temperature of the free surface of the drop, T_s is the temperature of the external air, and the temperature T_s is measured with a thermal imager. The equilibrium partial pressure of water vapor and the value of the vapor density are determined from the temperature of the free surface of the drop T_s.

Based on the above analysis, diagrams illustrating the influence of various factors on the evaporation of a drop are presented in Figure 14.
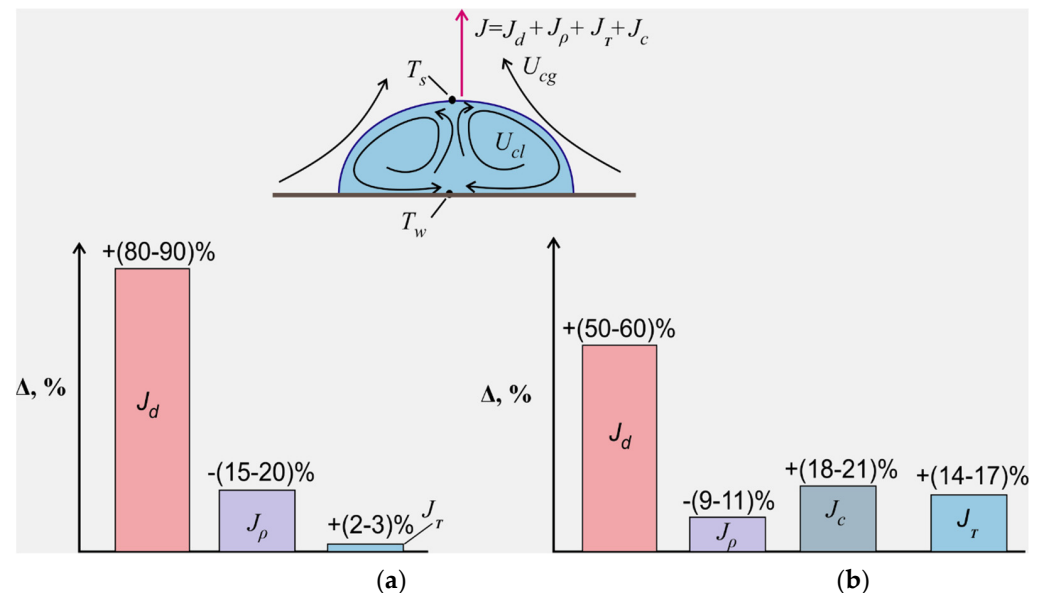

Figure 14. Influence of key factors on droplet evaporation, $\Delta = 100\% (J_{w,s} - J_w)/J_w$. (a) $T_w = 20$–21 °C, (b) $T_w = 90$ °C. Key: J_w (kg/s) —pure water mass flux, $J_{w,s}$ —solution mass flux for surfactant concentration of 10,000 ppm, J_d—drop diameter effect, J_ρ—partial pressure of water vapor effect, J_c—thermogravitational convection effect, and J_T—nonisothermality effect.

In Figure 14, the influence of various factors is denoted as follows: J_d is the influence of the droplet diameter, J_ρ is the influence of the equilibrium partial pressure of water vapor, J_c is the influence of thermogravitational convection, and J_T is the influence of nonisothermality. Both at $T_w = 20$ °C and at $T_w = 90$ °C, the predominant effect on evaporation is the growth of the droplet diameter due to the surfactant (J_d). At high temperature, J_c and J_T are comparable. The decrease in the evaporation rate (J_ρ) as a result of a decrease in the partial pressure of vapor at room temperature is double that at high-temperature heating. As the temperature T_s increases, the effect of J_ρ on evaporation decreases. The influence of the natural convection of gas ($J_c \sim (R_d)^{0.5}$) in Equation (5) noticeably manifests itself at high temperatures only (in Figure 10b, 18–21%) and at room temperature, thermogravitational convection can be neglected. As the wall temperature increases from 20 °C to 90 °C, the effect of J_T on the enhancement of evaporation increases approximately six times (from 2–3% to 14–17%). Thus, the $J/2R_d$ inversion with increasing wall temperature (when comparing the evaporation rate of a water drop and a drop of water with surfactant) is associated with a strong dependence of all these key factors on temperature.

At $T_w = 90$ °C, the experimental points $J/2R_d$ are located 67–71% above the calculated curves. According to Figure 14b, the influence of gas convection leads to a 67–70% excess of the experimental values of $J/2R_d$, compared to the calculated diffusion model (Equation 12), if the measured free surface temperature T_s is taken for the diffusion model. As mentioned above, 40% corresponds to an increase in the evaporation rate due to the buoyancy of water vapor. In Figure 14, this factor is not specified, since it has the same effect on a water drop with or without a surfactant. The increase in the evaporation rate due to thermogravitational convection is approximately 30% (40% + 30% = 70%). The effect of nonisothermality is expressed in a decrease in temperature T_s compared to the wall

temperature T_w. Thus, for T_w = 90, 60, 40, and 21 °C, the average temperature for the droplet surface T_s is approximately 78–80 °C, 54–55 °C, 38–39 °C, and 19–19.5 °C, respectively. At the maximum wall temperature (T_w), the decrease in ρ_{vs} due to the decrease in T_s is 40–50% (the maximum effect of nonisothermality on droplet evaporation).

At T_w = 60 °C, the influence of convection and nonisothermality decreases. At T_w = 40 °C, the calculation is slightly lower than the experimental points. During evaporation without heating (T_w = 20 °C), the Rayleigh number for the gas and liquid phases is low (there is no natural convection, since there is a small droplet height and small temperature gradients due to droplet evaporation), and the experimental data are quite accurately modeled by the diffusion model.

5. Conclusions

An experimental study of the evaporation of sessile drops of aqueous solutions with surfactant under nonisothermal conditions has been carried out. The choice of an immobile liquid drop as the object of study enabled the behavior of the contact line of three phases to be investigated, and the flow of an evaporating liquid to be measured over a wide temperature range from 20 °C to 90 °C. Using the optical method, droplet contact angles, droplet heights and contact diameters of evaporating droplets were measured in the temperature range.

An analysis of the contact diameter of the evaporating droplets has shown that pure water and weakly concentrated solutions on a copper substrate are characterized by fixed contact lines (so-called pinning). However, for a highly concentrated solution (above critical micelle concentration), pinning of the droplets under study was absent. At the initial stage, when the droplet was heated, an intense increase in the droplet diameter was observed.

Surfactant presence has a complex effect on the rate of a droplet's evaporation due to several factors, some of which decrease the evaporation rate while others, vice versa, increase it:

- The largest effect on the increase in the evaporation rate of a droplet is associated with an increase in its diameter due to a decrease in surface tension.
- It is shown that the evaporation of the surfactant solution layer is slower than for a pure water layer due to the drop in the partial vapor pressure. The magnitude of the effect depends on the substrate temperature. At room temperature, the decrease in the evaporation rate is 15–20%, and for a high-temperature substrate, the change is 9–11%.
- The contribution of nonisothermality increases by a factor of six as the substrate temperature rises from 20 °C to 90 °C.
- The effect of natural gas convection is significant only for nonisothermal evaporation with a contribution of about 20%.
- The effect of free gas convection leads to an excess of the experimental values of $J/2R_d$ by 67–70% compared to the calculated diffusion model.
- The effect of surfactants on the specific evaporation rate is inverted with an increase in the substrate temperature. In the isothermal case, the surfactant solution evaporates more slowly than pure water. In the nonisothermal case, the solution evaporates faster than pure water. This is due to the different dependence of key factors on temperature.

Author Contributions: Conceptualization, S.M. and I.V.; methodology, A.S. and V.M.; software, A.S. and Y.P.; validation, S.M., V.M. and I.V.; formal analysis, S.M.; investigation, A.S., Y.P. and V.M.; resources, Y.P.; data curation, S.M. and I.V.; writing—original draft preparation, S.M. and I.V.; writing—review and editing, S.M.; visualization, V.M. and A.S.; supervision, S.M.; project administration, I.V.; funding acquisition, I.V. All authors have read and agreed to the published version of the manuscript.

Conflicts of Interest: The authors declare no conflict of interest.

Nomenclature

α	Heat transfer coefficient
β	Convective mass transfer coefficient
β_T	The thermal liquid expansion
λ	Thermal conductivity
λ_c	Capillary length
σ	Surface tension
μ	Dynamic viscosity
ν	Kinematic viscosity
ρ_g	Gas density
ρ_l	Liquid density
ρ_{vs}	Vapor density on the droplet interface
ρ_a	Atmospheric density
ρ_{va}	Vapor density in the ambient atmosphere
θ	Contact angle
τ_e	Characteristic time of evaporation
Δm	The change in mass
Δt	Period of time
ΔT_s	The temperature difference between the temperature of the droplet interface and the temperature of the ambient air
ΔT_w	The temperature difference between the wall temperature and the droplet interface temperature
g	Gravitational acceleration
p_v	Partial vapor pressure
q_l	Total heat flux in the liquid
q_e	Evaporative heat flux
q_r	Radiative heat flux
q_c	Natural convection heat flux
r	Latent heat of vaporization
h	Droplet height
a	Thermal diffusivity
j	Specific mass transfer rate
J	Evaporation rate
S_d	Drop surface
V_d	Drop volume
R_d	Drop radius
F	The interface area of the liquid layer
L	The characteristic length of the diffusion vapor layer
B_M	Spalding mass transfer number
T	Temperature
T_a	Ambient atmosphere temperature
T_s	Droplet surface temperature
T_w	Substrate temperature
U_ρ	The vapor convection velocity
M_v	Vapor molar mass
U_{cl}	The average convective velocity in the droplet
U_{ca}	The air velocity due to thermogravitational convection
RH	Relative humidity
Ma	Marangoni number
Nu	Nusselt number
Ra	Rayleigh number
Re	Reynolds number
Sh	Sherwood number
Sc	Schmidt number

References

1. Smakulski, P.; Pietrowicz, S. A review of the capabilities of high heat flux removal by porous materials, microchannels and spray cooling techniques. *Appl. Therm. Eng.* **2016**, *104*, 636–646. [CrossRef]
2. Wang, J.X.; Guo, W.; Xiong, K.; Wang, S.N. Review of aerospace-oriented spray cooling technology. *Prog. Aerosp. Sci.* **2020**, *116*, 100635. [CrossRef]
3. Zhang, J.; Zhang, S.; Chunhua, W.; Xiaoming, T. Recent advances in film cooling enhancement: A review. *Chin. J. Aeronaut.* **2020**, *33*, 1119–1136. [CrossRef]
4. Khan, M.G.; Fartaj, A. A review on microchannel heat exchangers and potential applications. *Int. J. Energy Res.* **2011**, *35*, 553–582. [CrossRef]
5. Smakulski, P.; Ishimoto, J.; Pietrowicz, S. The cooling performance of the micro-solid nitrogen spray technique on the cryopreservation vitrification process: A qualitative study. *Int. J. Heat Mass Transf.* **2022**, *184*, 122253. [CrossRef]
6. Pandya, N.S.; Shah, H.; Molana, M.; Tiwari, A.K. Heat transfer enhancement with nanofluids in plate heat exchangers: A comprehensive review. *Eur. J. Mech.-B/Fluids* **2020**, *81*, 173–190. [CrossRef]
7. Gandomkar, A.; Kalan, K.; Vandadi, M.; Shafii, M.; Saidi, M. Investigation and visualization of surfactant effect on flow pattern and performance of pulsating heat pipe. *J. Therm. Anal. Calorim.* **2020**, *139*, 2099–2107. [CrossRef]
8. Deegan, R.D.; Bakajin, O.; Dupont, T.F.; Huber, G.; Nagel, S.R.; Witten, T.A. Capillary flow as the cause of ring stains from dried liquid drops. *Nature* **1997**, *389*, 827–829. [CrossRef]
9. Cahile, M.; Benichou, O.; Cazabat, A. Evaporating droplets of completely wetting liquids. *Langmuir* **2002**, *18*, 7985–7990. [CrossRef]
10. Shahidzadeh-Bonn, N.; Rafai, S.; Azouni, A.; Bonn, D. Evaporating droplets. *J. Fluid Mech.* **2006**, *549*, 307–313. [CrossRef]
11. Bonn, D.; Eggers, J.; Indekeu, J.; Meunier, J.; Rolley, E. Wetting and spreading. *Rev. Mod. Phys.* **2009**, *81*, 739. [CrossRef]
12. Maxwell, J.C. *Diffusion, Collected Scientific Papers*; Encyclopedia Britannica: Cambridge, UK, 1877.
13. Fuchs, N.A.; Pratt, J.N.; Sabersky, R.H. Evaporation and droplet growth in gaseous media. *J. Appl. Mech.* **1960**, *27*, 759–760. [CrossRef]
14. Tonini, S.; Cossali, G. An analytical model of liquid drop evaporation in gaseous environment. *Int. J. Therm. Sci.* **2012**, *57*, 45–53. [CrossRef]
15. Hu, H.; Larson, R.G. Evaporation of a sessile droplet on a substrate. *J. Phys. Chem. B* **2002**, *106*, 1334–1344. [CrossRef]
16. Gatapova, E.Y.; Semenov, A.A.; Zaitsev, D.V.; Kabov, O.A. Evaporation of a sessile water drop on a heated surface with controlled wettability. *Colloids Surf. A Physicochem. Eng. Asp.* **2014**, *441*, 776–785. [CrossRef]
17. Shekriladze, I.G. Boiling heat transfer: Mechanisms, models, correlations and the lines of further research. *Open Mech. Eng. J.* **2008**, *2*, 104–127. [CrossRef]
18. Erbil, H.Y. Control of stain geometry by drop evaporation of surfactant containing dispersions. *Adv. Colloid Interface Sci.* **2015**, *222*, 275–290. [CrossRef] [PubMed]
19. Tarasevich, Y.Y. Simple analytical model of capillary flow in an evaporating sessile drop. *Phys. Rev. E* **2005**, *71*, 027301. [CrossRef] [PubMed]
20. Ait Saada, M.; Chikh, S.; Tadrist, L. Numerical investigation of heat and mass transfer of an evaporating sessile drop on a horizontal surface. *Phys. Fluids* **2010**, *22*, 112115. [CrossRef]
21. Timm, M.L.; Dehdashti, E.; Darban, A.J.; Masoud, H. Evaporation of a sessile droplet on a slope. *Sci. Rep.* **2019**, *9*, 19803. [CrossRef]
22. Misyura, S. The dependence of drop evaporation rate and wettability on corrosion kinetics. *Colloids Surf. A Physicochem. Eng. Asp.* **2021**, *610*, 125735. [CrossRef]
23. Misyura, S.Y.; Volkov, R.S.; Filatova, A.S. Interaction of two drops at different temperatures: The role of thermocapillary convection and surfactant. *Colloids Surf. A* **2018**, *559*, 275–283. [CrossRef]
24. Misyura, S.Y. The influence of convection on heat transfer in a water layer on a heated structured wall. *Int. Commun. Heat Transf.* **2019**, *102*, 14–21. [CrossRef]
25. Truskett, V.N.; Stebe, K.J. Influence of surfactants on an evaporating drop: Fluorescence images and particle deposition patterns. *Langmuir* **2003**, *19*, 8271–8279. [CrossRef]
26. Kim, D.O.; Rokoni, A.; Kaneelil, P.; Cui, C.; Han, L.H.; Sun, Y. Role of surfactant in evaporation and deposition of bisolvent biopolymer droplets. *Langmuir* **2019**, *35*, 12773–12781. [CrossRef] [PubMed]
27. Semenov, S.; Trybala, A.; Agogo, H.; Kovalchuk, N.; Ortega, F.; Rubio, R.G.; Starov, V.M.; Velarde, M.G. Evaporation of droplets of surfactant solutions. *Langmuir* **2013**, *29*, 10028–10036. [CrossRef]
28. Guti'errez, G.; Benito, J.M.; Coca, J.; Pazos, C. Vacuum evaporation of surfactant solutions and oil-in-water emulsions. *Chem. Eng. J.* **2010**, *162*, 201–207. [CrossRef]
29. Guo, D.S.; Li, X.B.; Zhang, H.N.; Li, F.C.; Ming, P.J.; Oishi, M.; Oshima, M. Experimental study on the characteristics of temperature dependent surface/interfacial properties of a non-ionic surfactant aqueous solution at quasi-thermal equilibrium condition. *Int. J. Heat Mass Transf.* **2022**, *182*, 122003. [CrossRef]
30. Abe, Y.; Iwasaki, A.; Tanaka, K. Microgravity experiments on phase change of self-rewetting fluids. *Ann. N. Y. Acad. Sci.* **2004**, *1027*, 269–285. [CrossRef]

31. Suzuki, K.; Nakano, M.; Itoh, M. Subcooled Boiling of Aqueous Solution of Alcohol. In Proceedings of the 6th KSME-JSME Joint Conference on Thermal and Fluid Engineering Conference, Jeju City, Republic of Korea, 20–23 March 2005; pp. 21–23.
32. Savino, R.; Cecere, A.; Di Paola, R. Surface tension-driven flow in wickless heat pipes with self-rewetting fluids. *Int. J. Heat Fluid Flow* **2009**, *30*, 380–388. [CrossRef]
33. Savino, R.; Cecere, A.; Van Vaerenbergh, S.; Abe, Y.; Pizzirusso, G.; Tzevelecos, W.; Mojahed, M.; Galand, Q. Some experimental progresses in the study of self-rewetting fluids for the SELENE experiment to be carried in the Thermal Platform 1 hardware. *Acta Astronaut.* **2013**, *89*, 179–188. [CrossRef]
34. Hu, Y.; Liu, T.; Li, X.; Wang, S. Heat transfer enhancement of micro oscillating heat pipes with self-rewetting fluid. *Int. J. Heat Mass Transf.* **2014**, *70*, 496–503. [CrossRef]
35. Semenov, A.; Peschenyuk, Y.A.; Vozhakov, I. Application of Aqueous Solutions of Surfactants in Pulsating Heat Pipe. *J. Eng. Thermophys.* **2021**, *30*, 58–63. [CrossRef]
36. Sobac, B.; Brutin, D. Thermal effects of the substrate on water droplet evaporation. *Phys. Rev. E* **2012**, *86*, 021602. [CrossRef] [PubMed]
37. Kutateladze, S. *Fundamentals of Heat Transfer Theory*; Atomizdat: Moscow, Russia, 1979; p. 416.
38. Misyura, S.Y. Dependence of wettability of microtextured wall on the heat and mass transfer: Simple estimates for convection and heat transfer. *Int. J. Mech. Sci.* **2020**, *170*, 105353. [CrossRef]
39. Misyura, S.; Morozov, V.; Egorov, R. Water evaporation on structured surfaces with different wettability. *Int. J. Heat Mass Transf.* **2022**, *192*, 122843. [CrossRef]
40. Volkov, R.; Strizhak, P.; Misyura, S.; Lezhnin, S.; Morozov, V. The influence of key factors on the heat and mass transfer of a sessile droplet. *Exp. Therm. Fluid Sci.* **2018**, *99*, 59–70. [CrossRef]
41. Carrier, O.; Shahidzadeh-Bonn, N.; Zargar, R.; Aytouna, M.; Habibi, M.; Eggers, J.; Bonn, D. Evaporation of water: Evaporation rate and collective effects. *J. Fluid Mech.* **2016**, *798*, 774–786. [CrossRef]
42. Dunn, G.; Wilson, S.; Duffy, B.; David, S.; Sefiane, K. The strong influence of substrate conductivity on droplet evaporation. *J. Fluid Mech.* **2009**, *623*, 329–351. [CrossRef]
43. Doganci, M.D.; Sesli, B.U.; Erbil, H.Y. Diffusion-controlled evaporation of sodium dodecyl sulfate solution drops placed on a hydrophobic substrate. *J. Colloid Interface Sci.* **2011**, *362*, 524–531. [CrossRef]
44. Zhang, J.; Wang, B. Study on the interfacial evaporation of aqueous solution of SDS surfactant self-assembly monolayer. *Int. J. Heat Mass Transf.* **2003**, *46*, 5059–5064. [CrossRef]